Fock-Darwin States of Dirac Electrons in Graphene-Based Artificial Atoms

Hong-Yi Chen,[1] Vadim Apalkov,[2] and Tapash Chakraborty[1]

[1]*Department of Physics and Astronomy, University of Manitoba, Winnipeg, MB R3T 2N2, Canada*
[2]*Department of Physics and Astronomy, Georgia State University, Atlanta, Georgia 30303, USA*

(Received 16 November 2006; published 1 May 2007)

We investigate the Fock-Darwin states of the massless chiral fermions confined in a graphitic parabolic quantum dot. In light of Klein tunneling, we analyze the condition for confinement of the Dirac fermions in a cylindrically symmetric potential. New features of the energy levels of the Dirac electrons as compared to the conventional electronic systems are discussed. We also evaluate the dipole-allowed transitions in the energy levels of the dots. We propose that in the high magnetic field limit, the band parameters can be accurately determined from the dipole-allowed transitions.

DOI: 10.1103/PhysRevLett.98.186803 PACS numbers: 73.63.Kv, 05.30.Fk, 81.05.Uw

Quantum dots (QDs), or the ''artificial atoms'' [1] are one of the most intensely studied systems in condensed matter physics where the fundamental effects related to various quantum phenomena in confined geometries can be studied but with the unique advantage that the nature of the confinement and the electron density can be tuned externally. However, much of the interest in this system derives from its enormous potentials for applications, ranging from novel lasers to quantum information processing. While the majority of the QD systems investigated are based on the semiconductor heterostructures, in recent years, quantum dots created in the carbon nanotubes have been reported in the literature where the ''atomic'' properties [2] were clearly elucidated and its importance in technological applications was also demonstrated [3]. Conductance properties of ultrathin graphitic QDs [4] have also been reported recently. It is now well recognized that the low-energy dynamics of the two-dimensional electrons in graphene is governed by the Dirac-Weyl equation, and the charge carriers behave as massless chiral fermions [5,6]. In this situation, confinement of electrons becomes quite a challenging task, due to the so-called Klein paradox [7]. This problem has been dealt with in the case of a one-dimensional (1D) wire at zero field [8–10] and at finite [11] magnetic fields. In this Letter, we report on the electronic properties of the parabolic QDs in graphene. In particular, we present the energy levels as a function of the magnetic field (Fock-Darwin states [1]) and the associated dipole-allowed optical transitions in this system. We propose that the optical spectroscopy of the graphene QD in the high-field limit could provide an accurate means of determining the band parameters of graphene.

The Hamiltonian of a single electron in graphene with a cylindrically symmetric confinement potential is

$$\mathbf{H} = \mathbf{H}_0 + \mathbf{H}_1 = \frac{\gamma}{\hbar}(\vec{\sigma}\,\vec{\pi}) + V(r), \tag{1}$$

where $\vec{\sigma}$ are the Pauli matrices, $\vec{\pi} = \vec{p} + \frac{e}{c}\vec{A}$, $\vec{A} = \frac{B}{2} \times (-y, x)$ is the vector potential corresponding to the magnetic field B in the z direction orthogonal to the graphene plane, and $\gamma = \sqrt{3}a\gamma_0/2$ is the band parameter. Here $a = 0.246$ nm is the lattice constant and γ_0 (meV) is the transfer integral between the nearest-neighbor carbon atoms [12]. Properties of such systems have been studied intensively for the massive relativistic electrons [13], for which there are bound states in the external potential.

First we analyze the properties of the graphene system in the absence of a magnetic field to find the condition for confinement of an electron in the potential $V(r)$. Because of Klein tunneling the electrons in graphene cannot be localized by a confinement potential, since for any potential there will be the electron states with negative energy (the hole states) which would provide the escape channel for the electron inside the potential well. We can then discuss only the quasilocalized states or trapping of the electron by the confinement potential. This problem has been treated for the quasi-1D graphene system [8,14], where it was shown that the transverse momentum in 1D introduces the classically forbidden regions, which helps in trapping the electron. The width of the quasilocalized level is determined by the tunneling through the classically forbidden regions. For the zero transverse momentum, the tunneling barriers disappear and there are no trapped states. In our case, we have a cylindrically symmetric confinement potential with the effective transverse momentum m/r, where m is the electron angular momentum. Therefore, for $m \neq 0$ we expect the trapping of an electron by a cylindrically symmetric QD. In terms of the two-component wave function $(\chi_1(r)e^{i(m-1)\theta}, \chi_2(r)e^{im\theta})$, the Schrödinger equation corresponding to the Hamiltonian (1) is

$$V(r)\chi_1 - i\gamma\frac{d\chi_2}{dr} - i\gamma\frac{m}{r}\chi_2 = E\chi_1, \tag{2}$$

$$V(r)\chi_2 - i\gamma\frac{d\chi_1}{dr} + i\gamma\frac{m-1}{r}\chi_1 = E\chi_2. \tag{3}$$

There are no analytical solutions to these equations; therefore, we first present below a semiclassical analysis.

Semiclassical analysis.—At a large m we seek a solution of Eqs. (2) and (3) in the form e^{iqr}, which gives

$$(E - V/\gamma)^2 = (m/r)^2 + q^2. \tag{4}$$

The classical turning points can be found from the condition $q = 0$, and the classical region is $|E - V(r)| > \gamma|m|/r$. If r_0 is the solution of the equation $E - V(r) = 0$ then we can find the classically forbidden region as $(r_0 - \Delta r) < r < (r_0 + \Delta r)$, where $\Delta r = m/Fr_0$, $F = \gamma^{-1}dV(r_0)/dr$, and we assumed that $F \gg m/r_0^2$. If the electron is trapped in the dot, i.e., at $r < r_0 - \Delta r$, then the escape rate or the width of the quasilocalized levels is determined by tunneling through the classically forbidden region,

$$T = \exp\left(-\int_{r_0-\Delta r}^{r_0+\Delta r} |q(r)|dr\right) = \exp\left(-\frac{\pi m^2}{2Fr_0^2}\right). \quad (5)$$

Therefore, in order to trap the electron we need a large m and a small F, i.e., a smooth confinement potential. For a potential $V = (u/n)r^p$, Eq. (5) takes the form

$$T = \exp\left[-\frac{\pi\gamma m^2}{2ur_0^{p+1}}\right] = \exp\left[-\frac{\pi m^2}{p(E/\epsilon_p)^{p+1/p}}\right], \quad (6)$$

where $\epsilon_p = (\gamma^p u/p)^{1/(p+1)}$. Equation (6) gives the upper limit on the energy of the quasilocalized levels at a given m, i.e., $E/\epsilon_p < m^{2p/(p+1)}$. Based on the semiclassical expression we can also find the interlevel separation of the quasilocalized levels at large energies, $\Delta E_p = \alpha\epsilon_p(E/\epsilon_p)^{-1/p}$, where $\alpha \sim 1$. We then estimate the number of quasilocalized levels $N_{p,m}$ for a given angular momentum m and a given potential profile from $N_{p,m} = \int_0^{m^{2p/(p+1)}} \frac{dE}{\Delta E_p} \sim \frac{p}{p+1}m^2$. This estimation is valid for large m. For a small m we need to solve the system of equations (2) and (3) numerically to find the properties of the quasilocalized states.

Quasilocalized states: Numerical solutions.—At small m, the system of equations (2) and (3) can be solved only numerically. To extract the information about the width of the quasibound levels we need to impose special boundary conditions far from the QD. This condition means that far from the origin, $r \gg r_0$, the solution should be an outgoing wave, i.e., the propagation away from the QD [15]. Clearly [Eqs. (2) and (3)] for $r \gg r_0$ the outgoing solution is

$$\chi_1(r) = -\chi_2(r) = C\exp\left(\frac{i}{\gamma}\int^r V(r')dr'\right), \quad (7)$$

where C is a constant. Equation (7) is the boundary condition for the system (2) and (3) at large distances. Since at $r = 0$ the solution should be nondivergent, another boundary condition is $\chi_1(r = 0) = \chi_2(r = 0) = 0$. A solution with these boundary conditions exists only for a complex energy E. The imaginary part of the energy determines the width of the quasilocalized level.

We have solved Eqs. (2) and (3) numerically for a potential of the form $V(r) = (\frac{u}{p})r^p$ for different values of the exponent, p, and for different values of the angular momentum m. In dimensionless units, i.e., for the units of length and the energy, $a_p = (p\gamma/u)^{1/(p+1)}$ and $\epsilon_p = (\gamma^p u/p)^{1/(p+1)}$, respectively. By numerically solving Eqs. (2) and (3) we want to illustrate the formation of the quasilocalized states at small m and find the values of the angular momentum when we should expect the trapping of an electron by the QD. The results are shown in Fig. 1, where only the states with the smallest imaginary part of the energies, i.e., a small width of the levels, are shown. These states are the quasilocalized states of the QD. The manifestation of such states can be found already at $m = 2$ (circles), both for $p = 2$ [Fig. 1(a)] (parabolic) and $p = 4$ [Fig. 1(b)]. The strength of the localization can be characterized in terms of the ratio of Im(E) to the interlevel spacing. For $m = 2$ this ratio is 50. With an increase of the angular momentum the quasilocalized states become well developed and at $m = 10$ we clearly see the states with very low Im(E). The ratio of Im(E) to the interlevel spacing for these states is about 800, while for $m = 5$ this ratio is about 200. With an increase of the energy the states are less localized; i.e., Im(E) increases and is consistent with Eq. (6). Note that for all values of the exponent p there are no localized states at $m = 1$ [inset of Fig. 1(a)]. All the states at $m = 1$ have very large Im(E). There are also no quasilocalized states at $m = 0$. The reason for delocalization of the electron at $m = 0$ and 1 is that the effective transverse momentum for either the χ_1 component (at $m = 0$) or the χ_2 component (at $m = 1$) is zero. Based on the results shown in Fig. 1, we conclude that already at $m > 5$ we can observe trapping of the electron by the QD. At a

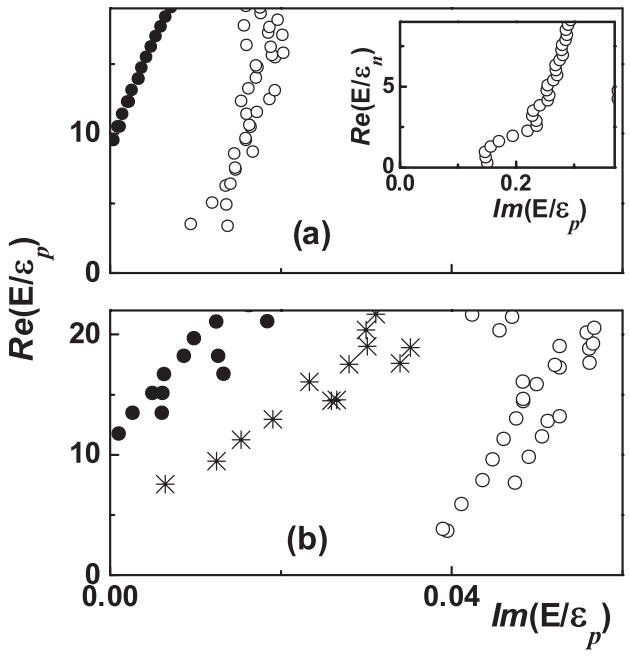

FIG. 1. The real and imaginary parts of the energy spectra of an electron in a QD with a confinement potential $V(r) = (u/p)r^p$, shown for various values of the exponent p and the angular momentum m: (a) $p = 2$, $m = 2$ (open circles), and $p = 2$, $m = 10$ (solid circles); (b) $p = 4$, $m = 2$ (open circles), $p = 4$, $m = 5$ (stars), and $p = 4$, $m = 10$ (solid circles). The results for $p = 2$ and $m = 1$ are shown in the inset. The energy is in units of ϵ_p.

smaller angular momentum the electron will be almost delocalized. In what follows, we analyze the magnetic field effects on the electronic states of the QDs.

Magnetic field: Semiclassical analysis.—In a magnetic field, the system of equations (2) and (3) has an additional nondiagonal term proportional to the magnetic field. In the dimensionless units, i.e., for the units of length a_p and the energy ϵ_p, the system is characterized by only one parameter, $b = (eB/2c)(p\gamma/u)^{2/(p+1)}$. In the semiclassical approximation, the effective transverse momentum is $(m/r + br)$ and Eq. (4) becomes $T = \exp[-\pi(m + b\tilde{E}^{2/p})^2/p\tilde{E}^{p+1/p}]$, where $\tilde{E} = E/\epsilon_p$. The effect of the magnetic field is different for the states with a positive or a negative m (the sign of m depends on the direction of a magnetic field). For a positive m the application of a magnetic field increases the effective transverse momentum and suppresses the tunneling from the QD. For a negative m, the magnetic field *decreases* the transverse momentum. Therefore the state becomes less localized. If we increase the magnetic field even further then at some point, $b = m/\tilde{E}^{2/p}$, the level becomes *delocalized*, and at an even larger B the level again becomes localized. Now the trapping will be due to the magnetic field. Therefore for a negative m, the magnetic field induces a *localization-delocalization-localization* transition. The physical origin of this effect is in the specific feature of localization of a relativistic electron in a confinement potential. The localization is due to the presence of the transverse momentum which produces the trapping barrier. Without a magnetic field this transverse momentum is due to the electron angular momentum m. Magnetic field introduces an additional rotation of the electron. If this rotation is opposite to the rotation due to m then at first the magnetic field suppresses the localization and then it becomes the main source of the electron rotation that results in the localization.

The number of the quasilocalized states in a weak magnetic field is estimated to be $N_{p,m} \sim [m + b|m|^{2/(p+1)}]^2$. This number with a positive m increases with an increasing magnetic field, while that for a negative m decreases with the magnetic field up to a certain value of B and then increases. The total number of states with positive and negative angular momenta, $N_{p,m} + N_{p,-m} \sim m^2 + b^2|m|^{4/(p+1)}$, always increases with an increasing B. From this behavior we expect the following effect: We assume that the QD is occupied by electrons up to a certain energy; i.e., the states with both positive and negative angular momenta are occupied and the net angular momentum of the dot is zero. We then apply a magnetic field and the states with positive m become more localized while the electrons from the states with negative m will escape from the QD. Finally, the electrons in the QD will have a net positive angular momentum and correspondingly a net magnetic moment.

Magnetic field: Numerical results.—To study the dependence of the quasilocalized spectra on the magnetic field we introduce the wave functions of the Hamiltonian $\mathbf{H}_0$, i.e., without a confinement potential [16], as the basis functions. To eliminate any escape of the electron from the QD we consider only the basis functions with positive energy,

$$\Psi_{n,m} = C_N \begin{pmatrix} \mathrm{sgn}(N)\phi_{n,m-1}(x) \\ i\phi_{n,m}(x) \end{pmatrix}, \tag{8}$$

where $N = n + \frac{1}{2}(|m| + m)$ is the Landau level (LL) index, $C_{N=0} = 1$ and $C_{N\neq 0} = 1/\sqrt{2}$, $\mathrm{sgn}(N = 0) = 0$, and $\phi_{n,m}$ is the Landau wave function [1]. Here $L_n^{|m|}(x)$ is the associated Laguerre polynomial, $x = r^2/a'^2$ is a dimensionless distance, and a' is the characteristic length of the system. Without the confinement, a' should be equal to the magnetic length $l = \sqrt{\hbar c/eB}$. In the presence of the parabolic confinement, the Hamiltonian suggests a natural unit of length $(\gamma/u)^{1/3}$ [8] and a natural unit of energy $(\gamma^2 u)^{1/3}$. This length characterizes the size of a parabolic dot in graphene. Therefore, $2/a'^2 = 1/l^2 + (u/\gamma)^{2/3}$.

In our numerical calculations, we choose the band parameter to be $\gamma = 646$ meV nm for $\gamma_0 = 3.03$ eV [17]. The low-lying energy states of the graphene QD are shown in Fig. 2. The results shown in Fig. 2 look different from the results in Fig. 1 because in Fig. 2 we have suppressed any escape from QD and, hence, only the lowest trapped states but not the escape from them are considered. In the absence of a confinement potential, the Dirac spectrum scales as $\sqrt{2}\gamma\sqrt{N}/l$ (shown as the inset of Fig. 2). In the Fock-Darwin spectrum for a conventional electron dot, the energy levels are degenerate and equally spaced at $B = 0$ [1]. The two-dimensional parabolic confinement considered here shows two outstanding features in contrast to the Fock-Darwin spectra at $B = 0$. The first is the lifting of the degeneracy and the other is the unequal separation among the energy levels. Figure 2 shows the field-dependent energy spectrum for $u = 0.1$. The energy difference between the lowest two levels at $B = 0$ is about

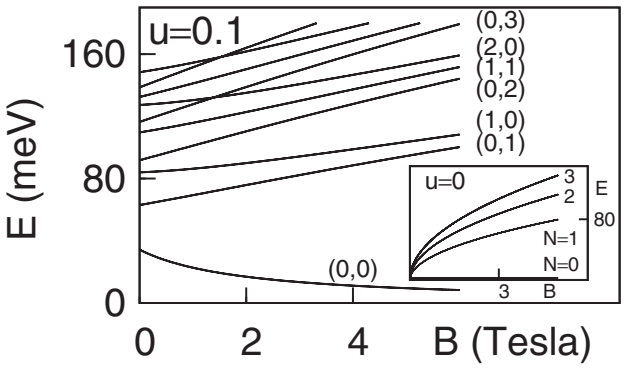

FIG. 2. Fock-Darwin spectrum of the Dirac quantum dots, plotted for the confinement potential strength $u = 0.1$ (meV/nm^2). The numbers in the parentheses correspond to the two quantum numbers n and m. Results for $u = 0$ are given in the inset.

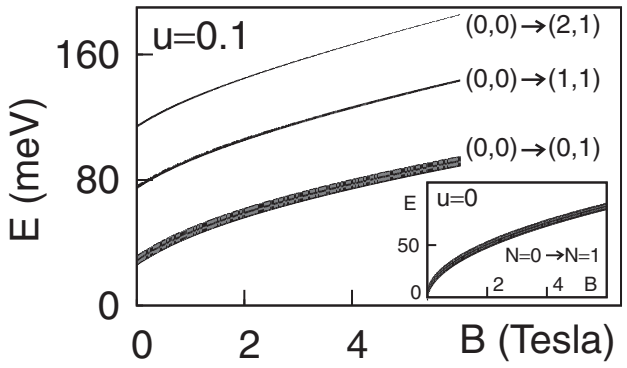

FIG. 3. The dipole-allowed transitions in the Fock-Darwin spectrum of graphene QDs for $u = 0.1$. Inset: the case of $u = 0$. The thickness of the lines is proportional to the calculated intensity. From the bottom to the top, the relative intensities are about 1.0, 0.1, 0.02, respectively.

$(\gamma^2 u)^{1/3}$. At a low magnetic field, the magnetic length l is larger than or comparable to the size of the confinement $(\gamma/u)^{1/3}$ and there is a hybridization of the LLs with the levels arising from the spatial confinement. In the high magnetic field limit $l \ll (\gamma/u)^{1/3}$, the Landau-type levels prevail, as expected. The Fock-Darwin spectra for conventional quantum dots have been determined earlier by the transport spectroscopy [18]. Similar studies for the graphene QDs would be very important to explore the energy levels and the nature of confinement for Dirac fermions in a graphene QD.

Figure 3 shows the dipole-allowed optical absorption spectra [1,19] for $u = 0$ and $u = 0.1$. Without any confinement there is only the $(0, 0) \rightarrow (0, 1)$ transition (shown as the inset of Fig. 3). The additional transitions, $(0, 0) \rightarrow (1, 1)$ and $(0, 0) \rightarrow (2, 1)$, are due to the presence of the parabolic confinement. For the Dirac fermions in a QD, the lowest dipole-allowed transition is

$$\Delta E \simeq (\gamma^2 u)^{1/3} + \frac{\sqrt{2}\gamma}{l}. \tag{9}$$

For $B = 0$ the corresponding energy is $\approx (\gamma^2 u)^{1/3}$. As the magnetic field increases, ΔE approaches the cyclotron energy $\sqrt{2}\gamma/l = \sqrt{2}(e\gamma B/\hbar c)$, where γ can therefore be uniquely determined experimentally. Conventionally, in the nearest-neighbor tight-binding model, γ_0 is obtained by fitting the *ab initio* calculation and the experimental data [12]. In a GaAs quantum dot, the magnetic-field-dependent far-infrared absorption experiments have established the energy relation $\Delta E_{\pm} = \hbar\Omega \pm \frac{1}{2}\hbar\omega_c$ to a great accuracy [19]. Similarly, for the massless chiral fermions in a graphene QD, we expect that the band parameter γ can also be determined quite accurately by the optical absorption experiments in the high-field limit.

Although the high magnetic field results are the major focus of this Letter, as in this case the localization of the electron in a QD at all values of the m is provided by the magnetic field, at $B = 0$ the chiral nature of the states prevent the electrons from being confined in a QD. This clearly indicates that the nature of the energy states and the optical spectra at a very small B are still important open questions.

We would like to thank P. Pietiläinen and Xue-Feng Wang for helpful discussions. The work has been supported by the Canada Research Chair Program, a Canadian Foundation for Innovation grant, and the NSERC Discovery grant.

[1] T. Chakraborty, *Quantum Dots* (Elsevier, Amsterdam, 1999); T. Chakraborty, Comments Condens. Matter Phys. **16**, 35 (1992).
[2] M. R. Buitelaar *et al.*, Phys. Rev. Lett. **88**, 156801 (2002); D. H. Cobden and J. Nygård, *ibid.* **89**, 046803 (2002); S. Moriyama *et al.*, *ibid.* **94**, 186806 (2005); S.-H. Ke, H. U. Baranger, and W. Yang, *ibid.* **91**, 116803 (2003).
[3] K. Ishibashi *et al.*, J. Vac. Sci. Technol. A **24**, 1349 (2006).
[4] J. Scott Bunch *et al.*, Nano Lett. **5**, 287 (2005).
[5] K. S. Novoselov *et al.*, Nature (London) **438**, 197 (2005); Y. Zhang *et al.*, *ibid.* **438**, 201 (2005).
[6] T. Ando, in *Nano-Physics & Bio-Electronics: A New Odyssey*, edited by T. Chakraborty, F. Peeters, and U. Sivan (Elsevier, Amsterdam, 2002), Chap. 1.
[7] M. I. Katsnelson, K. S. Novoselov, and A. K. Geim, Nature Phys. **2**, 620 (2006); O. Klein, Z. Phys. **53**, 157 (1929); **41**, 407 (1927); A. Calogeracos and N. Dombey, Contemp. Phys. **40**, 313 (1999).
[8] P. G. Silvestrov and K. B. Efetov, Phys. Rev. Lett. **98**, 016802 (2007).
[9] B. Trauzettel *et al.*, Nature Phys. **3**, 192 (2007).
[10] L. Brey and H. A. Fertig, Phys. Rev. B **73**, 235411 (2006).
[11] N. M. R. Peres, A. H. Castro Neto, and F. Guinea, Phys. Rev. B **73**, 241403 (2006); A. De Martino, L. Dell'Anna, and R. Egger, Phys. Rev. Lett. **98**, 066802 (2007).
[12] R. Saito, G. Dresselhaus, and M. S. Dresselhaus, *Physical Properties of Carbon Nanotubes* (Imperial College, London, 1998).
[13] Q.-G. Lin, quant-ph/9910044; D-H. Lin, J. Math. Phys. (N.Y.) **47**, 042302 (2006), and references therein.
[14] V. V. Cheianov and V. I. Falko, Phys. Rev. B **74**, 041403 (2006).
[15] E. E. Narimanov *et al.*, Phys. Rev. Lett. **83**, 4991 (1999).
[16] Y. Zheng and T. Ando, Phys. Rev. B **65**, 245420 (2002).
[17] T. Ando, J. Phys. Soc. Jpn. **75**, 074716 (2006).
[18] P. L. McEuen *et al.*, Phys. Rev. Lett. **66**, 1926 (1991); J. Weis *et al.*, Phys. Rev. B **46**, 12 837 (1992); T. Schmidt *et al.*, *ibid.* **51**, 5570 (1995); S. Tarucha *et al.*, Phys. Rev. Lett. **77**, 3613 (1996).
[19] C. Sikorski and U. Merkt, Phys. Rev. Lett. **62**, 2164 (1989); B. Meurer, D. Heitmann, and K. Ploog, Phys. Rev. Lett. **68**, 1371 (1992); D. Heitmann and J. Kotthaus, Phys. Today **46**, No. 6, 56 (1993).